A Case of Solid-state Isomerism for a Rhodium Carbonyl Cluster Anion. Synthesis, Characterization in Solution and *X*-Ray Crystallographic Structures of the Salts $[NMe_4]_3[Rh_{11}(CO)_{23}]\cdot Me_2CO$ and $[NMe_4]_3[Rh_{11}(CO)_{23}]\cdot C_6H_5Me$†

Alessandro Fumagalli* and Secondo Martinengo
C.N.R. Centro di Studio per la Sintesi e la Struttura dei Composti dei Metalli di Transizione nei Bassi Stati di Ossidazione, Via G. Venezian 21, 20133 Milano, Italy
Gianfranco Ciani* and Angelo Sironi
Istituto di Chimica Strutturistica Inorganica, Via G. Venezian 21, 20133 Milano, Italy
Brian T. Heaton
Department of I.P.I. Chemistry, P.O. Box 149, University of Liverpool, Liverpool L69 3BX

Two crystal species, $[NMe_4]_3[Rh_{11}(CO)_{23}]\cdot Me_2CO$ (**1**) and $[NMe_4]_3[Rh_{11}(CO)_{23}]\cdot C_6H_5Me$ (**2**), containing two isomers of the same anion, have been isolated and investigated. The salt (**1**) crystallizes in the monoclinic space group $P2_1/n$, with $a = 12.275(4)$, $b = 19.987(5)$, $c = 24.007(5)$ Å, $\beta = 104.47(3)°$, and $Z = 4$; the salt (**2**) gives monoclinic crystals, space group $P2_1/c$, with $a = 19.545(2)$, $b = 12.597(2)$, $c = 24.151(2)$ Å, $\beta = 92.62(1)°$, and $Z = 4$. The structures were solved and refined on the basis of 7 421 [(**1**)] and 3 531 [(**2**)] significant counter data, converging to final *R* values of 0.032 and 0.041, respectively. The metallic skeleton (of ideal D_{3h} symmetry) is the same in the two species, based on three face-to-face condensed octahedral units, sharing a common edge, coincident with the ideal three-fold axis. The carbonyl stereochemistry however is different in (**1**) and (**2**), as well as the pattern of metal–metal bonds. Complexes (**1**) and (**2**) have identical i.r. spectra in solution and variable-temperature ^{13}C n.m.r. spectra show that the ligands are completely fluxional, even at −90 °C.

In a previous communication[1] we reported the preliminary results of the characterization of an unusual eleven-metal cluster species crystallized as $[NMe_4]_3[Rh_{11}(CO)_{23}]\cdot Me_2CO$ (**1**). Further studies on the chemistry of this anion led us to examine, by *X*-ray diffraction, other crystal samples of its $[NMe_4]^+$ salt. One of these, $[NMe_4]_3[Rh_{11}(CO)_{23}]\cdot C_6H_5Me$ (**2**), obtained by recrystallization of (**1**) from MeCN and toluene, revealed the existence of another isomeric structure for the same anion with a different carbonyl stereochemistry. This is uncommon and there are very few other examples of carbonyl clusters which exhibit solid-state isomerism, *e.g.* $[Ru_4H_3(CO)_{12}]^-$,[2] $[Os_3Pt(\mu\text{-}H)_2(\mu\text{-}CH_2)(CO)_{10}\{P(cyclo\text{-}C_6H_{11})_3\}]$,[3] and $[Ir_6(CO)_{16}]$.[4] It should be noted that, whereas the two different isomers of $[Ru_4H_3(CO)_{12}]^-$ and $[Os_3Pt(\mu\text{-}H)_2(\mu\text{-}CH_2)(CO)_{10}\{P(cyclo\text{-}C_6H_{11})_3\}]$ can also be detected by n.m.r. in solution, the two forms of $[Ir_6(CO)_{16}]$ appear rather stable and not easily interconverted. On the other hand, i.r. spectra in solution of both forms of $[Rh_{11}(CO)_{23}]^{3-}$ are identical as well as ^{13}C n.m.r. spectra which show that all the carbonyls are scrambling even at −90 °C; this facile ligand mobility indicates that there is a low activation energy pathway available for the interconversion of the two isomers found in the solid state. An analogous case of solid-state isomerism, resulting on recrystallization from different solvents, was found for $[Pt_3(\mu\text{-}PPh_2)_3Ph(PPh_3)_2]$,[5] which exists in two forms with different metallic skeletons. The two structures of $[Rh_{11}(CO)_{23}]^{3-}$ now reported are therefore the first example of isomerism due to different arrangements of carbonyl ligands in the solid state, induced by relatively small *differences in packing forces*. It seems very probable, however, that several cases of this type of isomerism will emerge in the future.‡

In order to compare *X*-ray data collected under the same conditions and on the same diffractometer, we have also reinvestigated the structure of compound (**1**). In this paper, we report full details of the synthesis and reactivity of the anion, the *X*-ray single-crystal structural determinations of the two species (**1**) and (**2**), and the spectroscopic characterization in solution, including variable-temperature ^{13}C n.m.r. measurements.

Results and Discussion

Synthesis of the $[Rh_{11}(CO)_{23}]^{3-}$ *Anion.*—The anion $[Rh_{11}(CO)_{23}]^{3-}$ was first obtained by oxidation of $[Rh_7(CO)_{16}]^{3-}$[6] in MeCN under nitrogen. The most convenient preparation used $FeCl_3$ as oxidant, in slight excess over the 1:1 molar ratio. The reaction appears to be consistent with the overall stoicheiometry shown in equation (1).

$$11[Rh_7(CO)_{16}]^{3-} + 12\,Fe^{3+} \longrightarrow 7[Rh_{11}(CO)_{23}]^{3-} + 12\,Fe^{2+} + 15\,CO \quad (1)$$

By monitoring the course of the reaction by i.r. it has been possible to identify several steps; the nature and relative amounts of the intermediate species depend upon the rate of addition of the oxidant. In fact, if Fe^{3+} is added in small portions the gradual disappearance of $[Rh_7(CO)_{16}]^{3-}$ with formation of $[Rh_9(CO)_{19}]^{3-}$[7] and $[Rh_{12}(CO)_{30}]^{2-}$[8] is seen before the formation of $[Rh_{11}(CO)_{23}]^{3-}$, which is the main product at the stoicheiometry shown in equation (1).

† Tris(tetramethylammonium) 1,3;2,4;3,4;1,7;2,8;9,5;3,11;7,8;6,9;11,4;10,7;10,8-dodeca-μ-carbonyl-3,4,5,5,6,6,7,8,9,10,11-undecacarbonyl-*cyclo*-undecarhodate–acetone (1/1) (28 *Rh–Rh*) and tris(tetramethylammonium) 1,3;2,4;1,5;3,4;1,7;2,6;9,4;3,11;6,9;7,8;10,6;10,8;11,7-trideca-μ-carbonyl-3,4,5,5,6,7,8,9,10,11-decacarbonyl-*cyclo*-undecarhodate–toluene (1/1) (28 *Rh–Rh*) respectively.

Supplementary data available: see Instructions for Authors, *J. Chem. Soc., Dalton Trans.*, 1988, Issue 1, pp. xvii—xx.

‡ It has recently been found that the solid-state structure of $[NMe_2(CH_2Ph)_2][Ir_4(CO)_{11}(SCN)]$ has all the CO ligands terminally bound, whereas in solution and in the solid state with other cations the anion always adopts a structure with bridging carbonyls (R. DellaPergola, L. Garlaschelli, F. Demartin, M. Manassero, M. Sansoni, and S. Martinengo, unpublished work).

The anion $[Rh_{11}(CO)_{23}]^{3-}$ is also formed on reacting mixtures of smaller clusters, provided that the ratio of total anionic charge:metal atoms is correct. Examples of such reactions are shown in equations (2)—(4). Reactions (1) and (2)

$$[Rh_7(CO)_{16}]^{3-} + [Rh_4(CO)_{12}] \longrightarrow [Rh_{11}(CO)_{23}]^{3-} + 5\,CO \quad (2)$$

$$2[Rh_4(CO)_{12}] + 3[Rh(CO)_4]^- \longrightarrow [Rh_{11}(CO)_{23}]^{3-} + 13\,CO \quad (3)$$

$$[Rh_6(CO)_{15}]^{2-} + [Rh_5(CO)_{15}]^- \longrightarrow [Rh_{11}(CO)_{23}]^{3-} + 7\,CO \quad (4)$$

are more convenient because of the ready availability of the reactants.[6,9] However, although reaction (3) is more critical because it requires the use of $[Rh(CO)_4]^-$,[10] it is synthetically useful because it is possible to prepare $Na_3[Rh_{11}(CO)_{23}]$ from which a whole series of salts with different cations can be obtained by simple metathesis. Reaction (4), because of the laborious preparation of both reagents[6,11] is not convenient.

All the syntheses described above take several days to go to completion at room temperature; reaction times are shorter at higher temperature, but, due to the thermal instability of $[Rh_{11}(CO)_{23}]^{3-}$ (see later), 50 °C must not be exceeded; even at this moderate temperature the reaction is more critical, and the i.r. should be monitored closely to avoid excessive formation of by-products.

Very recently[12] the preparation of $[Rh_{11}(CO)_{23}]^{3-}$ through the stepwise cluster growth process shown in equation (5) has been reported.

$$[Rh_9(CO)_{19}]^{3-} \xrightarrow{[Rh(CO)_2(NCMe)_2]^+} [Rh_{10}(CO)_{21}]^{2-} \xrightarrow{[Rh(CO)_4]^-} [Rh_{11}(CO)_{23}]^{3-} \quad (5)$$

The $[Rh_{11}(CO)_{23}]^{3-}$ anion has been obtained as Na^+, $[NMe_4]^+$, $[N(PPh_3)_2]^+$, and $[NMe_3(CH_2Ph)]^+$ salts. The sodium salt is soluble in tetrahydrofuran (thf), acetone, ethyl methyl ketone, MeCN, and MeOH, while the bulky cations salts are soluble in acetone or MeCN and poorly soluble in thf and alcohols. From the point of view of purification $[NMe_4]^+$ is the best cation, because it allows a clean separation of $[Rh_{11}(CO)_{23}]^{3-}$ from the reaction by-products on crystallization of the crude salt from acetone and propan-2-ol; in this way large black crystals of (**1**) are obtained. Species (**2**), observed the first time by chance, is obtained from pure (**1**) on simple recrystallization from MeCN and toluene; the intermediate crystallization of (**1**) is in this case necessary because direct treatment of the crude $[NMe_4]^+$ salt in MeCN with toluene does not allow separation from the by-products.

Reactivity of $[Rh_{11}(CO)_{23}]^{3-}$.—The $[Rh_{11}(CO)_{23}]^{3-}$ anion belongs to a class of rhodium cluster compounds of medium nuclearity which includes $[Rh_9(CO)_{19}]^{3-}$,[8] $[Rh_{10}(CO)_{21}]^{2-}$,[12] and $[Rh_{12}H_2(CO)_{25}]$,[13] all based on metallic skeletons resulting from face-shared octahedral units. Due to the intermediate position between low-nuclearity species (up to seven metal atoms) and the larger, compact clusters, which contain at least one metal atom with entirely metallic coordination (13 and more metals), this medium-nuclearity class plays a key role in understanding the mechanism of cluster growth and thus is useful for the development of rational stepwise syntheses of higher nuclearity species. The $[Rh_{11}(CO)_{23}]^{3-}$ anion is thermally unstable, and easily yields higher nuclearity species through loss of CO; thus, a short reflux in MeCN (*ca.* 1 h) yields as the main product $[Rh_{14}(CO)_{25}]^{4-}$,[14] this result is not unexpected because both the starting and the resulting products have approximately the same anionic charge:metal atoms ratio (0.273 and 0.286, respectively). This allows the pyrolytic growth process to be regarded essentially as a thermally induced cleavage of M–CO bonds and formation of new M–M interactions.

The $[Rh_{11}(CO)_{23}]^{3-}$ anion is rather unreactive towards carbon monoxide at atmospheric pressure and only after 2—3 d under 4—5 atm of CO in MeCN solution is reaction observed to give smaller clusters according to equation (6), which is formally the reverse of equation (4). This allowed ^{13}CO-enriched samples to be obtained by direct exchange in acetone solution without significant decomposition since exchange is complete within 30 min.

$$[Rh_{11}(CO)_{23}]^{3-} + 7\,CO \longrightarrow [Rh_6(CO)_{15}]^{2-} + [Rh_5(CO)_{15}]^- \quad (6)$$

The $[Rh_{11}(CO)_{23}]^{3-}$ anion reacts slowly with excess of halide ions (Cl^-) in MeCN under nitrogen to give a mixture of products among which $[Rh(CO)_2Cl_2]^-$ and $[Rh_9(CO)_{19}]^{3-}$ have been identified.

Description of the Structures of $[Rh_{11}(CO)_{23}]^{3-}$, (**1**) *and* (**2**).—The structures of $[Rh_{11}(CO)_{23}]^{3-}$ for crystals containing acetone (**1**) and toluene (**2**) are shown in Figures 1 and 2, respectively. Bond parameters are reported in Table 1 for (**1**) and in Table 2 for (**2**). The anion contains a Rh_{11} metallic array, of ideal D_{3h} symmetry, which consists of three condensed octahedral units (see also Figure 3) having a common edge [Rh(1)–Rh(2)] coincident with the ideal three-fold axis. Each octahedral unit shares a face with both of the adjacent octahedra. The same metallic skeleton has also been found in the mixed-metal cluster $[Pt_2Rh_9(CO)_{22}]^{3-}$,[15] in which the Pt atoms occupy the sites with the maximum metal–metal connectivity [corresponding to Rh(1) and Rh(2)]. Since the dihedral angle between adjacent faces of a regular octahedron is 109° 28′, regular face-to-face condensation of three such units with a common edge leaves some 'unfilled space' which is avoided by

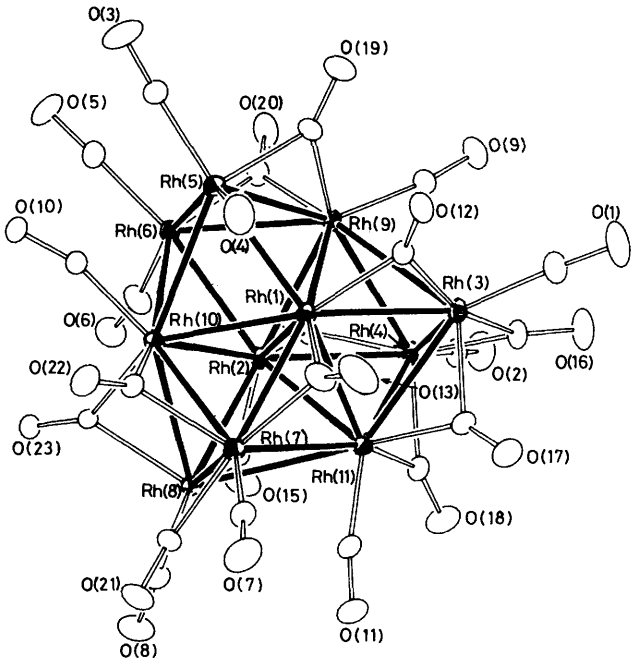

Figure 1. A view of the anion $[Rh_{11}(CO)_{23}]^{3-}$ in (**1**). The carbonyl ligands are indicated by the numbers of their oxygen atoms

Table 1. Bond distances (Å) and angles (°) within $[NMe_4]_3[Rh_{11}(CO)_{23}]\cdot Me_2CO$ (**1**)

Rh(1)–Rh(2)	2.964(1)	Rh(3)–Rh(9)	2.957(1)	Rh(3)–C(1)	1.90(1)	Rh(2)–C(15)	1.94(1)
Rh(1)–Rh(3)	2.720(1)	Rh(3)–Rh(11)	2.836(1)	Rh(4)–C(2)	1.90(1)	Rh(8)–C(15)	2.07(1)
Rh(1)–Rh(5)	2.685(1)	Rh(4)–Rh(9)	2.967(1)	Rh(5)–C(3)	1.88(1)	Rh(3)–C(16)	2.07(1)
Rh(1)–Rh(7)	2.730(1)	Rh(4)–Rh(11)	2.834(1)	Rh(5)–C(4)	1.89(1)	Rh(4)–C(16)	2.01(1)
Rh(1)–Rh(9)	2.797(1)	Rh(5)–Rh(6)	2.708(1)	Rh(1)···C(4)	2.45(1)	Rh(3)–C(17)	2.06(1)
Rh(1)–Rh(10)	2.731(1)	Rh(5)–Rh(9)	2.834(1)	Rh(6)–C(5)	1.88(1)	Rh(11)–C(17)	2.01(1)
Rh(1)–Rh(11)	2.756(1)	Rh(5)–Rh(10)	2.861(1)	Rh(6)–C(6)	1.91(1)	Rh(4)–C(18)	2.08(1)
Rh(2)–Rh(4)	2.723(1)	Rh(6)–Rh(9)	2.842(1)	Rh(7)–C(7)	1.91(1)	Rh(11)–C(18)	2.01(1)
Rh(2)–Rh(6)	2.701(1)	Rh(6)–Rh(10)	2.829(1)	Rh(8)–C(8)	1.92(1)	Rh(5)–C(19)	2.02(1)
Rh(2)–Rh(8)	2.699(1)	Rh(7)–Rh(8)	2.740(1)	Rh(9)–C(9)	1.90(1)	Rh(9)–C(19)	2.01(1)
Rh(2)–Rh(9)	2.744(1)	Rh(7)–Rh(10)	2.757(1)	Rh(10)–C(10)	1.87(1)	Rh(6)–C(20)	2.01(1)
Rh(2)–Rh(10)	2.738(1)	Rh(7)–Rh(11)	2.984(1)	Rh(11)–C(11)	1.86(1)	Rh(9)–C(20)	2.04(1)
Rh(2)–Rh(11)	2.761(1)	Rh(8)–Rh(10)	2.791(1)	Rh(1)–C(12)	1.99(1)	Rh(7)–C(21)	2.07(1)
Rh(3)–Rh(4)	2.725(1)	Rh(8)–Rh(11)	3.062(1)	Rh(3)–C(12)	2.05(1)	Rh(8)–C(21)	2.00(1)
				Rh(1)–C(13)	1.98(1)	Rh(7)–C(22)	2.04(1)
				Rh(7)–C(13)	2.06(1)	Rh(10)–C(22)	2.02(1)
				Rh(2)–C(14)	1.96(1)	Rh(8)–C(23)	2.11(1)
				Rh(4)–C(14)	2.11(1)	Rh(10)–C(23)	2.02(1)
C(1)–O(1)	1.14(1)	C(7)–O(7)	1.12(1)	C(12)–O(12)	1.15(1)	C(18)–O(18)	1.16(1)
C(2)–O(2)	1.11(1)	C(8)–O(8)	1.12(1)	C(13)–O(13)	1.16(1)	C(19)–O(19)	1.17(1)
C(3)–O(3)	1.13(1)	C(9)–O(9)	1.14(1)	C(14)–O(14)	1.17(1)	C(20)–O(20)	1.18(1)
C(4)–O(4)	1.14(1)	C(10)–O(10)	1.17(1)	C(15)–O(15)	1.17(1)	C(21)–O(21)	1.18(1)
C(5)–O(5)	1.12(1)	C(11)–O(11)	1.14(1)	C(16)–O(16)	1.19(1)	C(22)–O(22)	1.18(1)
C(6)–O(6)	1.11(1)			C(17)–O(17)	1.15(1)	C(23)–O(23)	1.13(1)
Rh(1)–Rh(5)–C(3)	167.1(3)	Rh(2)–Rh(6)–C(5)	169.8(3)	Rh(3)–C(1)–O(1)	171.9(8)	Rh(7)–C(7)–O(7)	175.4(8)
Rh(1)–Rh(5)–C(4)	62.0(4)	Rh(2)–Rh(6)–C(6)	71.3(3)	Rh(4)–C(2)–O(2)	178.6(8)	Rh(8)–C(8)–O(8)	177.7(8)
Rh(6)–Rh(5)–C(3)	99.8(3)	Rh(5)–Rh(6)–C(5)	93.9(3)	Rh(5)–C(3)–O(3)	177.3(8)	Rh(9)–C(9)–O(9)	172.8(7)
Rh(6)–Rh(5)–C(4)	148.1(3)	Rh(5)–Rh(6)–C(6)	156.9(3)	Rh(5)–C(4)–O(4)	157.8(10)	Rh(10)–C(10)–O(10)	162.3(6)
C(3)–Rh(5)–C(4)	105.4(5)	C(5)–Rh(6)–C(6)	100.3(4)	Rh(6)–C(5)–O(5)	178.6(7)	Rh(11)–C(11)–O(11)	170.1(7)
				Rh(6)–C(6)–O(6)	170.3(9)		
Rh(1)–C(12)–O(12)	138.8(6)	Rh(2)–C(15)–O(15)	139.1(6)	Rh(4)–C(18)–O(18)	132.1(7)	Rh(7)–C(21)–O(21)	133.9(7)
Rh(3)–C(12)–O(12)	136.7(6)	Rh(8)–C(15)–O(15)	136.3(6)	Rh(11)–C(18)–O(18)	140.2(7)	Rh(8)–C(21)–O(21)	141.2(7)
Rh(1)–C(12)–Rh(3)	84.4(3)	Rh(2)–C(15)–Rh(8)	84.5(3)	Rh(4)–C(18)–Rh(11)	87.7(3)	Rh(7)–C(21)–Rh(8)	84.8(3)
Rh(1)–C(13)–O(13)	138.1(7)	Rh(3)–C(16)–O(16)	135.0(6)	Rh(5)–C(19)–O(19)	134.2(6)	Rh(7)–C(22)–O(22)	134.7(5)
Rh(7)–C(13)–O(13)	136.9(6)	Rh(4)–C(16)–O(16)	140.5(6)	Rh(9)–C(19)–O(19)	136.5(6)	Rh(10)–C(22)–O(22)	139.9(5)
Rh(1)–C(13)–Rh(7)	85.0(3)	Rh(3)–C(16)–Rh(4)	84.0(3)	Rh(5)–C(19)–Rh(9)	89.3(3)	Rh(7)–C(22)–Rh(10)	85.5(3)
Rh(2)–C(14)–O(14)	141.8(6)	Rh(3)–C(17)–O(17)	131.6(6)	Rh(6)–C(20)–O(20)	137.0(6)	Rh(8)–C(23)–O(23)	132.0(5)
Rh(4)–C(14)–O(14)	134.1(5)	Rh(11)–C(17)–O(17)	140.0(7)	Rh(9)–C(20)–O(20)	133.8(6)	Rh(10)–C(23)–O(23)	142.4(5)
Rh(2)–C(14)–Rh(4)	84.0(3)	Rh(3)–C(17)–Rh(11)	88.2(3)	Rh(6)–C(20)–Rh(9)	89.2(3)	Rh(8)–C(23)–Rh(10)	85.0(2)

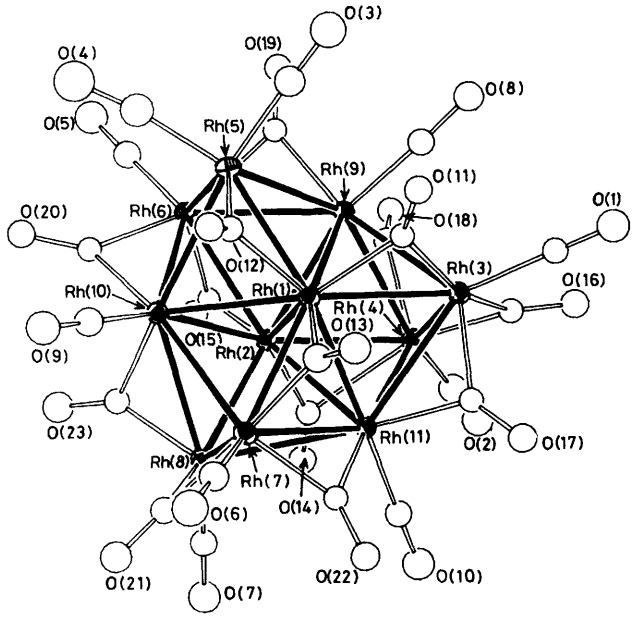

Figure 2. A view of the anion $[Rh_{11}(CO)_{23}]^{3-}$ in (**2**). The carbonyl ligands are indicated by the numbers of their oxygen atoms

distortion. This is seen by an analysis of the metal–metal bonds, which are rather scattered for both species: in the range 2.685(1)—3.062(1) Å in (**1**) and 2.659(2)—3.150(2) Å in (**2**). An analogous scattering of metal–metal bonds has been also observed in the isostructural cluster $[Pt_2Rh_9(CO)_{22}]^{3-}$ [range 2.654(3)—2.997(4) Å].[15]

Of the 28 M–M interactions, five in (**1**) [range 2.957(1)—3.063(1) Å] and four in (**2**) [range 2.948(2)—3.150(2) Å] (in both cases unbridged edges), are notably long, very probably because of the requirements mentioned above for the condensation of the three octahedra; in particular the interstitial edge Rh(1)–Rh(2) belongs to this class. The other metal–metal bonding distances in both species are distributed without any clear difference between bridged and unbridged edges.

Considering the metal polyhedron, there are three types of metals, with different metal–metal connectivities; seven for Rh(1) and Rh(2), six for Rh(9), Rh(10), and Rh(11) and four for the remaining Rh atoms.

The carbonyl distribution in the two different forms is quite different and the geometry of the 23 CO ligands in both species is such that the ideal D_{3h} cluster symmetry is drastically lowered. An approximate mirror plane, passing through Rh(9), Rh(10), and Rh(11), is maintained in (**1**) (ideal overall C_s symmetry), while in (**2**) no symmetry element is present (see Figure 3).

Table 2. Bond distances (Å) and angles (°) within $[NMe_4]_3[Rh_{11}(CO)_{23}]\cdot C_6H_5Me$ (**2**)

Rh(1)–Rh(2)	2.951(2)	Rh(3)–Rh(9)	2.861(2)	Rh(3)–C(1)	1.88(2)	Rh(2)–C(15)	1.96(2)
Rh(1)–Rh(3)	2.751(2)	Rh(3)–Rh(11)	2.861(2)	Rh(4)–C(2)	1.82(2)	Rh(6)–C(15)	2.02(2)
Rh(1)–Rh(5)	2.684(2)	Rh(4)–Rh(9)	2.804(2)	Rh(5)–C(3)	1.87(2)	Rh(3)–C(16)	2.03(2)
Rh(1)–Rh(7)	2.750(2)	Rh(4)–Rh(11)	2.954(2)	Rh(5)–C(4)	1.85(2)	Rh(4)–C(16)	1.95(2)
Rh(1)–Rh(9)	2.899(2)	Rh(5)–Rh(6)	2.754(2)	Rh(6)–C(5)	1.88(2)	Rh(3)–C(17)	1.98(2)
Rh(1)–Rh(10)	2.779(2)	Rh(5)–Rh(9)	2.887(2)	Rh(7)–C(6)	1.82(2)	Rh(11)–C(17)	2.03(2)
Rh(1)–Rh(11)	2.706(2)	Rh(5)–Rh(10)	2.832(2)	Rh(8)–C(7)	1.83(2)	Rh(4)–C(18)	2.00(2)
Rh(2)–Rh(4)	2.673(2)	Rh(6)–Rh(9)	2.848(2)	Rh(9)–C(8)	1.86(2)	Rh(9)–C(18)	2.04(2)
Rh(2)–Rh(6)	2.699(2)	Rh(6)–Rh(10)	2.787(2)	Rh(10)–C(9)	1.85(2)	Rh(6)–C(19)	2.16(2)
Rh(2)–Rh(8)	2.659(2)	Rh(7)–Rh(8)	2.683(2)	Rh(11)–C(10)	1.89(2)	Rh(9)–C(19)	1.99(2)
Rh(2)–Rh(9)	2.685(2)	Rh(7)–Rh(10)	3.150(2)	Rh(1)–C(11)	1.98(2)	Rh(6)–C(20)	2.05(2)
Rh(2)–Rh(10)	2.691(2)	Rh(7)–Rh(11)	2.891(2)	Rh(3)–C(11)	2.08(2)	Rh(10)–C(20)	1.98(2)
Rh(2)–Rh(11)	2.838(2)	Rh(8)–Rh(10)	2.777(2)	Rh(1)–C(12)	2.15(2)	Rh(7)–C(21)	2.16(2)
Rh(3)–Rh(4)	2.761(2)	Rh(8)–Rh(11)	2.948(2)	Rh(5)–C(12)	1.97(2)	Rh(8)–C(21)	1.89(2)
				Rh(1)–C(13)	2.03(2)	Rh(7)–C(22)	1.98(2)
				Rh(7)–C(13)	1.94(2)	Rh(11)–C(22)	2.00(2)
				Rh(2)–C(14)	1.86(2)	Rh(8)–C(23)	1.88(2)
				Rh(4)–C(14)	2.30(2)	Rh(10)–C(23)	2.12(2)
C(1)–O(1)	1.14(2)	C(6)–O(6)	1.18(2)	C(11)–O(11)	1.16(2)	C(18)–O(18)	1.20(2)
C(2)–O(2)	1.19(2)	C(7)–O(7)	1.15(2)	C(12)–O(12)	1.14(2)	C(19)–O(19)	1.17(2)
C(3)–O(3)	1.15(2)	C(8)–O(8)	1.16(2)	C(13)–O(13)	1.21(2)	C(20)–O(20)	1.22(2)
C(4)–O(4)	1.20(3)	C(9)–O(9)	1.16(2)	C(14)–O(14)	1.20(2)	C(21)–O(21)	1.21(2)
C(5)–O(5)	1.16(2)	C(10)–O(10)	1.13(2)	C(15)–O(15)	1.19(2)	C(22)–O(22)	1.21(2)
				C(16)–O(16)	1.21(2)	C(23)–O(23)	1.23(2)
				C(17)–O(17)	1.21(2)		
C(3)–Rh(5)–C(4)	93(1)	Rh(1)–C(11)–O(12)	138(1)	Rh(6)–C(15)–O(15)	135(1)	Rh(6)–C(19)–Rh(9)	86.7(7)
		Rh(3)–C(11)–O(12)	137(1)	Rh(2)–C(15)–Rh(6)	85.6(7)	Rh(6)–C(20)–O(20)	134(1)
Rh(3)–C(1)–O(1)	179(2)	Rh(1)–C(11)–Rh(3)	85.2(7)	Rh(3)–C(16)–O(16)	135(1)	Rh(10)–C(20)–O(20)	138(1)
Rh(4)–C(2)–O(2)	179(1)	Rh(1)–C(12)–O(12)	136(2)	Rh(4)–C(16)–O(16)	137(2)	Rh(6)–C(20)–Rh(10)	87.5(7)
Rh(5)–C(3)–O(3)	176(2)	Rh(5)–C(12)–O(12)	142(2)	Rh(3)–C(16)–Rh(4)	87.8(8)	Rh(7)–C(21)–O(21)	133(2)
Rh(5)–C(4)–O(4)	167(2)	Rh(1)–C(12)–Rh(5)	81.2(7)	Rh(3)–C(17)–O(17)	136(1)	Rh(8)–C(21)–O(21)	144(2)
Rh(6)–C(5)–O(5)	177(2)	Rh(1)–C(13)–O(13)	133(2)	Rh(11)–C(17)–O(17)	133(1)	Rh(7)–C(21)–Rh(8)	82.8(8)
Rh(7)–C(6)–O(6)	175(2)	Rh(7)–C(13)–O(13)	140(2)	Rh(3)–C(17)–Rh(11)	90.9(7)	Rh(7)–C(22)–O(22)	133(1)
Rh(8)–C(7)–O(7)	176(2)	Rh(1)–C(13)–Rh(7)	87.7(9)	Rh(4)–C(18)–O(18)	137(2)	Rh(11)–C(22)–O(22)	133(1)
Rh(9)–C(8)–O(8)	176(2)	Rh(2)–C(14)–O(14)	152(2)	Rh(9)–C(18)–O(18)	135(1)	Rh(7)–C(22)–Rh(11)	93(7)
Rh(10)–C(9)–O(9)	179(2)	Rh(4)–C(14)–O(14)	127(1)	Rh(4)–C(18)–Rh(9)	88.1(8)	Rh(8)–C(23)–O(23)	140(2)
Rh(11)–C(10)–O(10)	179(2)	Rh(2)–C(14)–Rh(4)	79.4(7)	Rh(6)–C(19)–O(19)	134(1)	Rh(10)–C(23)–O(23)	131(1)
		Rh(2)–C(15)–O(15)	139(1)	Rh(9)–C(19)–O(19)	139(1)	Rh(8)–C(23)–Rh(10)	87.8(8)

In (**1**) there are 12 almost symmetric edge-bridging groups (maximum of asymmetry 0.15 Å, mean Rh–C and C–O 2.03 and 1.17 Å respectively). The remaining 11 carbonyls are terminally bonded (mean Rh–C and C–O 1.89 and 1.13 Å, respectively); Rh(5) and Rh(6) bear two such ligands each, Rh(1) and Rh(2) none, and the remaining metal atoms one each. However one of these ligands, bound to Rh(5), exhibits a weak interaction with Rh(1) of 2.45(1) Å [*vs.* Rh(5)–C 1.89(1) Å], reflected also in the value of the Rh(5)–C–O angle of 157.8(10)°. This CO group might be alternatively described as quite asymmetric edge-bridging. Another very weak interaction is observed for the terminal CO bound to Rh(10) toward Rh(5) [Rh(5)–C 2.69(1) Å, Rh(10)–C–O 162.3(6)°].

In (**2**) there are 13 edge-bridging carbonyls spanning different situations: from almost symmetric (eight groups, maximum of asymmetry 0.10 Å, mean Rh–C and C–O 2.00 and 1.20 Å, respectively), to moderately asymmetric (four groups, maximum of asymmetry 0.27 Å, mean long Rh–C, short Rh–C, and C–O 2.15, 1.93, and 1.19 Å, respectively), to asymmetric bridges [one group, CO(14), Rh(2)–C(14) 1.86(2) Å, Rh(4)–C(14) 2.30(2) Å]. The 10 terminal carbonyl groups all show almost linear Rh–C–O interactions (mean Rh–C and C–O 1.86 and 1.16 Å, respectively); Rh(5) bears two such ligands, Rh(1) and Rh(2) none, and the other metals one each.

The two ligand stereochemistries represent two different modes of distributing the ligand-donated electrons so as to reach an almost homogeneous charge on all the cluster metals (principle of 'charge equalization'). The possibility of different ligand dispositions may be related to the cluster geometry, which exhibits a high number of co-ordination sites with respect to the number of ligands, thus determining a relatively low crowding on the surface. For instance, the octahedral species $[Rh_6C(CO)_{13}]^{2-}$,[16] $[Co_6C(CO)_{13}]^{2-}$,[17] and $[Co_6N(CO)_{13}]^{-}$[18] exhibit three different carbonyl arrangements.

The anion $[Pt_2Rh_9(CO)_{22}]^{3-}$, with the same type of metallic cluster, possesses a different carbonyl geometry which cannot be related to one of the two geometries presently found for the Rh_{11} species by simple removal of one CO group [Figure 3(*d*)]; interestingly, another recently characterized mixed-metal cluster species, $[Pt_3Rh_8(CO)_{22}]^{2-}$,[19] with the same metallic skeleton, presents a yet different ligand disposition.

Common features of the CO geometries in (**1**) and (**2**) are the following: (*i*) the central metals Rh(1) and Rh(2) do not bear terminal carbonyls (as for the two central Pt atoms in the Pt–Rh mixed-metal species), (*ii*) the metal atoms Rh(9), Rh(10), and Rh(11) each bear one terminal and two bridging carbonyls, (*iii*) none of the edges of class B [see Figure 3(*a*)] is bridged by a CO, probably because these edges are at the bottom of 'butterfly'-like cavities and a carbonyl bound there would give rise to some interactions also with the other adjacent metals (the two wing-tips of the 'butterfly').

The carbonyl geometries in (**1**) and (**2**) can be considered as two frozen steps of the fluxional process that occurs in solution. The interconversion energy must be low if relatively small

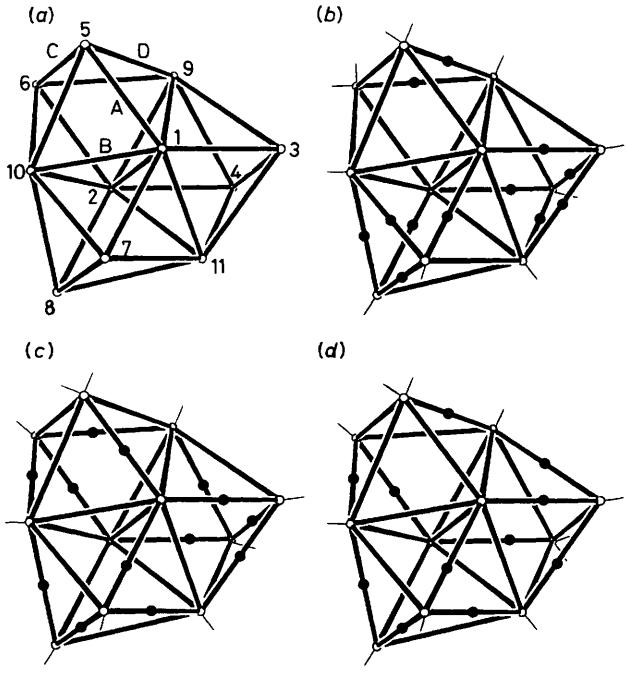

Figure 3. (*a*) The bare M_{11} cluster with atom numbering and the four classes of edges (A, B, C, and D) according to the ideal symmetry D_{3h}. (*b*) Schematic representation of the carbonyl distribution in (**1**). (*c*) Schematic representation of the carbonyl distribution in (**2**). (*d*) Schematic representation of the carbonyl distribution in $[Pt_2Rh_9(CO)_{22}]^{3-}$ (the Pt atoms are in the central positions 1 and 2)

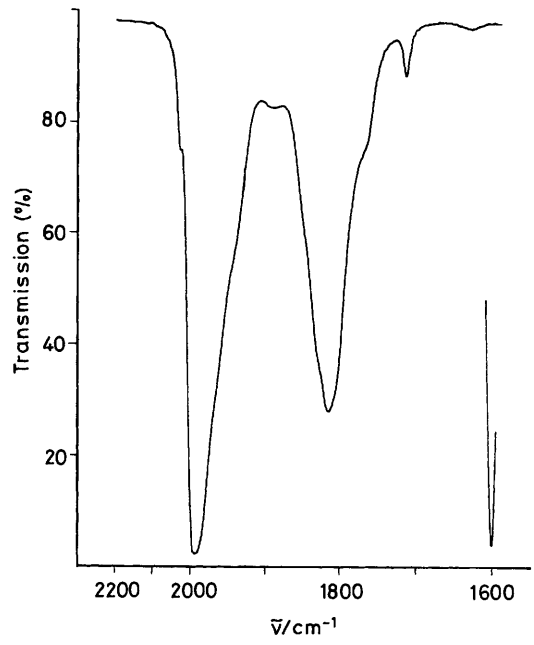

Figure 4. The ν(CO) region of the i.r. spectrum of $[NMe_4]_3[Rh_{11}(CO)_{23}]\cdot Me_2CO$ (**1**) in MeCN

differences in packing forces can stabilize different isomers in the solid state. Probably, in other packing environments (with different cations) new isomers might be isolated. The scrambling which makes all the ligands equivalent in solution (see below) can be rationalized, on the basis of the structural data, as a terminal–bridge–terminal interconversion involving all the surface edges of classes (A), (C), and (D) [Figure 3(*a*)], but probably not those of class (B). Though the central metals Rh(1) and Rh(2) in the two solid-state isomers do not bear terminal carbonyls the possibility that the above mechanism can operate in solution also within these metals can be inferred by the following observation. As mentioned above, a terminal CO in (**1**), bound to Rh(5), also exhibits a weak interaction with the nearest central metal atom; on the other hand in (**2**) one of the bridging ligands is quite asymmetric, showing a markedly shorter contact with a central metal. These two CO groups can therefore be regarded as two stages of the terminal–bridge–terminal passage from a peripheral to a central Rh atom or *vice versa*.

The anion possesses 148 valence electrons, corresponding to 74 cluster valence molecular orbitals (c.v.m.o.s). Some of us[20] have previously suggested that the more probable number of c.v.m.o.s for any compact closest-packed cluster, not flat and not exceedingly developed in one dimension, is $6N_{metals} + 7$. This has been verified in a variety of small, medium, and large compact clusters. It was also suggested that any decrease of compactness of the metallic array would require an increase of the number of c.v.m.o.s. The Rh_{11} skeleton is not compact closest-packed and can be seen as a sequence of three layers (3/5/3 metals): two outer triangles and a central triangle plus square. This implies a lowering of compactness in the central layer with respect to closest-packing and justifies the presence of one c.v.m.o. more than that required by the above rule. A similar decrease of compactness and increase of two c.v.m.o.s was discussed for the undecametal cluster, $[PtRh_{10}N(CO)_{21}]^{3-}$,[21] in relation to the presence of the interstitial nitride. A correct number of c.v.m.o.s for $[Rh_{11}(CO)_{23}]^{3-}$ is also predicted by the topological electron-counting theory.[22]

Spectroscopic Measurements.—The i.r. spectra in the carbonyl stretching region of compounds (**1**) and (**2**) are identical in MeCN solution, but (**1**) exhibits an extra band at 1 715w cm^{-1} due to clathrated acetone (Figure 4). Bands are at 2 032w, 1 995s, 1 890 vw, 1 817 ms and 1 770 (sh) cm^{-1}.

^{13}C N.m.r. spectra, recorded in $[^2H_6]$acetone for (**1**) and in $[^2H_3]$acetonitrile for (**2**), show, in the carbonyl region at room temperature, just the same single symmetrical complex resonance, whose centre lies at 214.8 and 214.5 p.p.m., respectively. Variable-temperature ^{13}C n.m.r. spectra of (**1**) in $[^2H_6]$acetone, show, throughout the range from −90 to +50 °C, always the same single resonance with some temperature-dependent shift in the range 216.1—214.5 p.p.m. Data acquisition under high resolution conditions (0.122 Hz) at room temperature gave the spectrum shown in Figure 5(*a*); this multiplet consists of a triplet of quartets of septets with J(Rh–C) of 5.38, 7.37, and 8.73 ± 0.25 Hz, respectively, due to all the carbonyls being equivalent and coupling to three sets of two, three, and six magnetically equivalent Rh atoms. The simulated ^{13}C n.m.r. spectrum, using this assignment, is shown in Figure 5(*b*). This implies that the metallic skeleton attains a much higher symmetry in solution (D_{3h}) through carbonyl migration and this is supported by direct ^{103}Rh n.m.r. measurements at −80 °C which show just three resonances at +636.6, −205.5, and +153.0 p.p.m. due to Rh(1,2), Rh(9,10,11), and the remaining Rh nuclei, respectively. The observed time-averaged values of J(Rh–C) thus decrease with increasing metal connectivity and it is worth noting that the rhodium resonance due to Rh(1,2) occurs at a significantly higher frequency region than the others. This region is tending towards that found for resonances due to interstitial rhodium nuclei[23] and is in keeping with Rh(1) and Rh(2) having the highest metal connectivity.

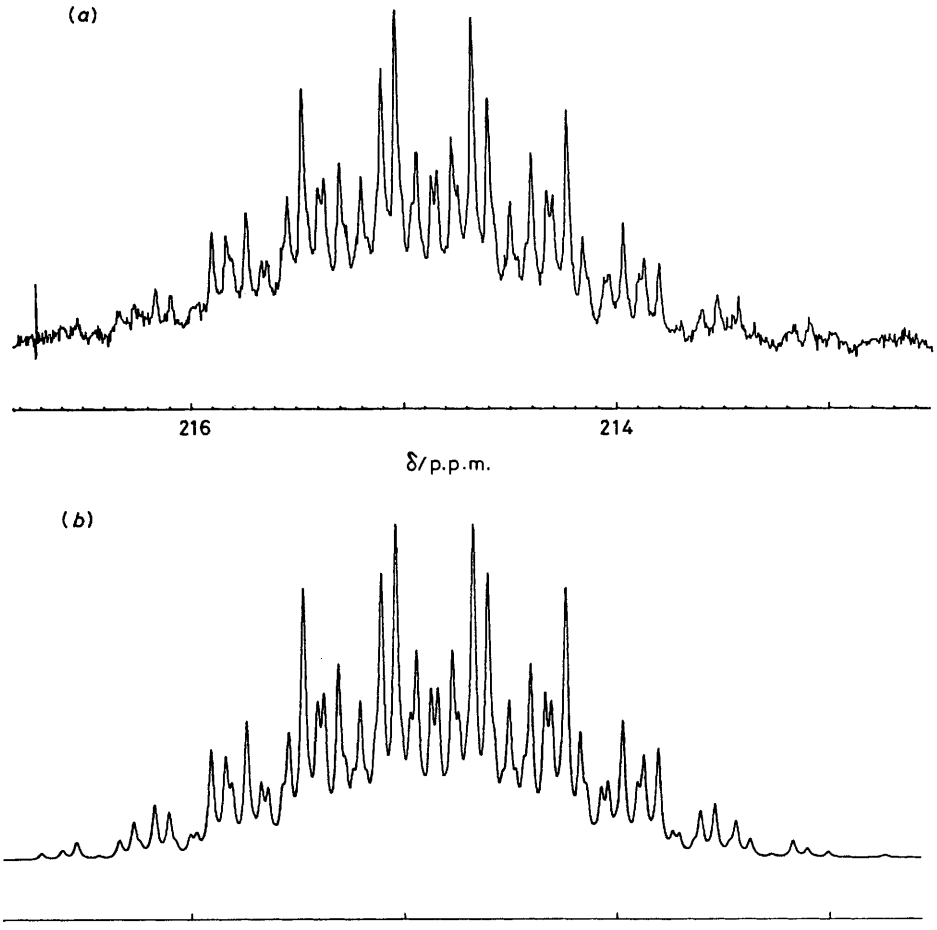

Figure 5. (*a*) ^{13}C N.m.r. spectrum of $[NMe_4]_3[Rh_{11}(CO)_{23}]$ (carbonyl region) in $[^2H_6]$acetone at room temperature. (*b*) Simulated spectrum with $J(Rh–C)$ = 5.38 (triplet), 7.37 (quartet), and 8.73 Hz (septet); $W_{\frac{1}{2}}$ = 0.6 Hz

Experimental

All the reactions and subsequent manipulations were carried out under a nitrogen atmosphere in carefully purified solvents using Schlenk-tube techniques. The complexes $[Rh_4(CO)_{12}]$,[9] $[Rh(CO)_4]^-$,[10] $[Rh_7(CO)_{16}]^{3-}$,[6] $[Rh_6(CO)_{15}]^{2-}$,[6] and $[Rh_5(CO)_{15}]^-$[11] were prepared according to the literature. The variable-temperature ^{13}C n.m.r. spectra were recorded on a Bruker WP 80 and direct ^{103}Rh spectra on a Bruker WH 360 spectrometer; $\delta(^{103}Rh)$ = 0 p.p.m. is related to a standard frequency (3.16 or 11.376 MHz) at such a magnetic field that the protons in $SiMe_4$ resonate at exactly 100 or 360 MHz, respectively.[24] Infrared spectra were recorded on a Perkin-Elmer 781 spectrophotometer using 0.1-mm CaF_2 cells previously purged with nitrogen.

Synthesis of $[Rh_{11}(CO)_{23}]^{3-}$.—(a) *From* $[Rh_7(CO)_{16}]^{3-}$ *and* $FeCl_3$. $[NMe_4]_3[Rh_7(CO)_{16}]$ (0.612 g, 0.44 mmol) in a 100-cm^3 Schlenk tube was dissolved in MeCN (8 cm^3) and treated with a 0.2 mol dm^{-3} solution of $FeCl_3$ in MeCN (2.4 cm^3, 0.48 mmol). The mixture was stirred at room temperature for 4 d, then filtered; the insoluble material, before being discarded, was washed with 2 cm^3 of MeCN. The solution and collected washings were treated with toluene (40 cm^3) which caused precipitation of an oily material, which eventually, upon concentration in vacuum, followed by addition of some more toluene (20 cm^3) and vigorous stirring, became microcrystalline. The mother-liquor, after decantation was removed with a syringe and the crude product (**2**) vacuum dried. Recrystallization was performed by redissolution in acetone (5 cm^3) and cautious layering of propan-2-ol (20 cm^3). When the diffusion was complete, the mother-liquor was removed and the product washed thoroughly with propan-2-ol. Yield: 0.360 g (63%) of product (**1**) as black crystals.

(b) *From* $[Rh_7(CO)_{16}]^{3-}$ *and* $[Rh_4(CO)_{12}]$. To $[NMe_4]_3[Rh_7(CO)_{16}]$ (0.763 g, 0.55 mmol) and $[Rh_4(CO)_{12}]$ (0.409 g, 0.55 mmol) under a nitrogen atmosphere in a 150-cm^3 Schlenk tube was added MeCN (20 cm^3). The mixture was stirred at room temperature for 5 d, and the brown solution was then evaporated to dryness by pumping in vacuum at room temperature. The residue was dissolved in acetone (15 cm^3) and the solution filtered; the insoluble residue was washed with a small amount of acetone (3 cm^3) and then discarded. The filtrate, together with the collected washing, was carefully layered with propan-2-ol (40 cm^3). After a few days the diffusion was complete and the black crystals of $[NMe_4]_3[Rh_{11}(CO)_{23}]\cdot Me_2CO$ were filtered off, washed with propan-2-ol and vacuum dried; yields 45—50% (Found: C, 22.00; H, 2.05; N, 1.95. Calc. for $C_{38}H_{42}N_3O_{24}Rh_{11}$: C, 22.20; H, 2.05; N, 2.05%). Addition of propan-2-ol to the mother-liquor allowed recovery of some other product (*ca.* 25%) in a microcrystalline form.

(c) *From* $[Rh_4(CO)_{12}]$ *and* $Na[Rh(CO)_4]$. To $[Rh_4(CO)_{12}]$ (0.473 g, 0.63 mmol) in thf (20 cm^3) in a 100-cm^3 Schlenk tube under nitrogen was added a 0.2 mol dm^{-3} solution in thf of $Na[Rh(CO)_4]$ (4.75 cm^3, 0.95 mmol) with stirring; the solution first turned green and then brown. Within the first 3 h of reaction the solution was briefly evacuated several times, in

order to remove the evolved CO, and then heated to 50 °C, monitoring closely the i.r. spectrum until the characteristic bands of $[Rh_{11}(CO)_{23}]^{3-}$ appeared (*ca.* 1 h). The vacuum dried mixture, upon redissolution in MeOH gave by metathesis with bulky cations the corresponding salts. However, apart from $[NMe_4]^+$, none of the cations tested gave a crystalline product.

Crystallization of $[NMe_4]_3[Rh_{11}(CO)_{23}]\cdot C_6H_5Me$.—$[NMe_4]_3[Rh_{11}(CO)_{23}]\cdot Me_2CO$ (0.160 g) was dissolved in MeCN (5 cm^3) and vacuum dried twice, to remove the clathrated acetone. The residue was redissolved in MeCN (5 cm^3) and the resulting solution carefully layered on toluene (15 cm^3) in a Schlenk tube. After a week, the precipitated product was filtered off, washed with toluene (2 × 5 cm^3), pentane (2 × 5 cm^3), and vacuum dried. Due to the unusual 'up-side down' diffusion process the product appeared mostly in a microcrystalline form with just a few crystals of a size suitable for *X*-ray diffraction studies. Yield *ca.* 0.08 g (Found: C, 23.90; H, 2.15; N, 1.80. Calc. for $C_{42}H_{44}N_3O_{23}Rh_{11}$: C, 24.15; H, 2.10; N, 2.00%).

Preparation of ^{13}CO*-enriched Samples.*—The ^{13}CO-enriched samples (*ca.* 20—25%) were prepared in two ways: (*a*) by direct exchange with 90% ^{13}CO using standard vacuum-line techniques, and (*b*) according to the above reported procedure from unenriched $[Rh_4(CO)_{12}]$ and enriched $[NMe_4]_3[Rh_7(CO)_{16}]$ (*ca.* 25%). The direct exchange was carried out as follows: a solution of $[NMe_4]_3[Rh_{11}(CO)_{23}]\cdot Me_2CO$ (0.297 g, 0.144 mmol) in acetone (5 cm^3) was stirred under ^{13}CO (44 cm^3, titre 90%) at room temperature. Monitoring the gaseous phase after 30 min showed that there had been a complete statistical exchange. The enriched product was recovered by addition of propan-2-ol to induce crystallization.

X-*Ray Analysis of Compounds* (**1**) *and* (**2**).—*Crystal data for* (**1**). $C_{38}H_{42}N_3O_{24}Rh_{11}$, M = 2 056.7, monoclinic, space group $P2_1/n$ (non-standard of no. 14), with a = 12.275(4), b = 19.987(5), c = 24.007(5) Å, β = 104.47(3)°, U = 5 703.1 Å^3, Z = 4, D_c = 2.395 g cm^{-3}, $F(000)$ = 3 912, Mo-K_α radiation (λ = 0.710 73 Å), and μ(Mo-K_α) = 31.24 cm^{-1}.

Crystal data for (**2**). $C_{42}H_{44}N_3O_{23}Rh_{11}$, M = 2 090.8, monoclinic, space group $P2_1/c$ (no. 14), a = 19.545(2), b = 12.597(2), c = 24.151(2) Å, β = 92.62(1)°, U = 5 940.0 Å^3, Z = 4, D_c = 2.338 g cm^{-3}, $F(000)$ = 3 984, Mo-K_α radiation (λ = 0.710 73 Å), and μ(Mo-K_α) = 30.00 cm^{-1}.

Intensity measurements. Crystal samples of dimensions 0.21 × 0.25 × 0.47 mm for (**1**) and 0.04 × 0.10 × 0.37 mm for (**2**) were mounted on glass fibres in air. The intensity data were collected for both species on an Enraf-Nonius CAD4 automated diffractometer, using graphite-monochromatized Mo-K_α radiation. The setting angles of 25 random intense reflections ($15 < 2\theta < 24°$) were used in each case to determine by least-squares fit accurate cell constants and orientation matrix. The data collections were performed by the ω-scan

Table 3. Final positional parameters within $[NMe_4]_3[Rh_{11}(CO)_{23}]\cdot Me_2CO$ (**1**)

Atom	*x*	*y*	*z*	Atom	*x*	*y*	*z*
Rh(1)	0.494 38(5)	0.252 27(3)	0.314 88(2)	O(14)	0.646 0(6)	−0.004 7(3)	0.382 1(2)
Rh(2)	0.630 02(5)	0.143 41(3)	0.382 37(2)	C(15)	0.788 4(7)	0.134 9(4)	0.421 5(4)
Rh(3)	0.516 42(5)	0.186 66(3)	0.219 05(2)	O(15)	0.857 9(5)	0.093 4(3)	0.432 7(3)
Rh(4)	0.644 29(5)	0.087 62(3)	0.280 95(2)	C(16)	0.596 3(7)	0.104 2(5)	0.195 8(3)
Rh(5)	0.328 96(5)	0.217 51(3)	0.364 19(3)	O(16)	0.597 9(6)	0.078 1(4)	0.151 4(3)
Rh(6)	0.453 88(5)	0.120 07(3)	0.428 27(2)	C(17)	0.650 4(7)	0.250 5(5)	0.224 0(4)
Rh(7)	0.655 72(5)	0.337 24(3)	0.374 84(2)	O(17)	0.670 0(6)	0.288 2(4)	0.191 4(3)
Rh(8)	0.778 06(5)	0.235 94(3)	0.437 87(2)	C(18)	0.791 5(7)	0.142 3(5)	0.287 8(3)
Rh(9)	0.425 91(5)	0.118 39(3)	0.307 14(2)	O(18)	0.879 5(5)	0.127 3(4)	0.282 8(3)
Rh(10)	0.549 32(4)	0.249 36(3)	0.432 35(2)	C(19)	0.270 0(7)	0.156 0(5)	0.296 5(4)
Rh(11)	0.709 05(5)	0.222 46(3)	0.306 67(2)	O(19)	0.181 5(5)	0.146 8(4)	0.265 5(3)
C(1)	0.441 7(8)	0.191 5(5)	0.139 7(4)	C(20)	0.394 9(7)	0.052 5(4)	0.366 1(3)
O(1)	0.403 9(7)	0.187 7(5)	0.091 4(3)	O(20)	0.355 8(6)	−0.001 8(3)	0.362 9(3)
C(2)	0.690 0(7)	0.000 5(5)	0.264 7(4)	C(21)	0.800 6(7)	0.334 9(6)	0.440 8(4)
O(2)	0.715 4(7)	−0.051 1(3)	0.255 8(3)	O(21)	0.862 9(6)	0.376 2(3)	0.465 2(3)
C(3)	0.196 9(7)	0.210 1(6)	0.389 8(4)	C(22)	0.558 8(6)	0.350 2(4)	0.431 9(3)
O(3)	0.115 1(6)	0.206 3(6)	0.403 1(4)	O(22)	0.526 8(5)	0.397 0(3)	0.453 0(3)
C(4)	0.324(1)	0.303 6(5)	0.331 4(4)	C(23)	0.683 5(6)	0.234 5(4)	0.499 9(3)
O(4)	0.294 3(7)	0.357 2(4)	0.321 0(3)	O(23)	0.707 3(5)	0.222 7(3)	0.547 6(2)
C(5)	0.350 0(8)	0.105 3(4)	0.472 9(4)	N(1)	0.459 6(6)	0.455 3(4)	0.113 3(3)
O(5)	0.288 2(6)	0.098 0(4)	0.499 8(3)	C(T11)	0.385 1(9)	0.396 9(6)	0.116 9(5)
C(6)	0.585 2(9)	0.079 5(5)	0.476 3(4)	C(T12)	0.407(1)	0.497 5(6)	0.061 6(5)
O(6)	0.652 7(6)	0.055 3(4)	0.509 6(3)	C(T13)	0.569(1)	0.431 0(8)	0.108 1(6)
C(7)	0.696 3(7)	0.426 7(4)	0.361 0(4)	C(T14)	0.466(1)	0.500 3(9)	0.165 4(7)
O(7)	0.722 7(6)	0.479 6(4)	0.356 7(3)	N(2)	−0.001 7(6)	0.322 4(4)	0.172 6(3)
C(8)	0.929 5(7)	0.227 7(5)	0.483 8(4)	C(T21)	0.042(1)	0.378 6(7)	0.214 7(6)
O(8)	0.016 2(6)	0.223 1(5)	0.512 2(4)	C(T22)	0.064(1)	0.324 8(6)	0.130 5(5)
C(9)	0.392 2(7)	0.059 6(4)	0.243 0(3)	C(T23)	−0.123(1)	0.332 8(6)	0.140 5(5)
O(9)	0.364 5(6)	0.021 0(4)	0.207 3(3)	C(T24)	0.017(1)	0.258 2(8)	0.203 9(7)
C(10)	0.439 3(6)	0.244 4(4)	0.473 6(3)	N(3)	0.181 3(7)	0.427 0(4)	0.471 8(3)
O(10)	0.388 6(5)	0.253 5(3)	0.507 9(2)	C(T31)	0.150(1)	0.425 0(8)	0.525 7(7)
C(11)	0.831 7(7)	0.280 2(5)	0.324 4(4)	C(T32)	0.100(1)	0.471 6(9)	0.434 4(7)
O(11)	0.910 7(5)	0.311 8(4)	0.328 4(3)	C(T33)	0.167(1)	0.362 3(9)	0.446 3(7)
C(12)	0.397 2(7)	0.251 0(4)	0.234 8(3)	C(T34)	0.297(1)	0.450 2(8)	0.482 1(7)
O(12)	0.315 5(5)	0.275 7(3)	0.208 4(2)	O(S1)	−0.051 1(8)	0.114 4(5)	0.111 0(4)
C(13)	0.535 0(8)	0.344 3(4)	0.297 9(4)	C(S1)	0.043(1)	0.085 8(7)	0.128 7(6)
O(13)	0.505 3(8)	0.384 4(3)	0.262 1(3)	C(S2)	0.059(1)	0.026 9(8)	0.166 3(6)
C(14)	0.639 0(7)	0.049 2(4)	0.362 1(3)	C(S3)	0.146(1)	0.117 1(8)	0.113 6(6)

method, within the limits $3 \leqslant \theta \leqslant 26°$ for (**1**) and $3 \leqslant \theta \leqslant 24°$ for (**2**). A variable scan speed (2—20° min^{-1}) and a variable scan range of $(a + 0.35 \tan \theta)°$ with $a = 1.0$ for (**1**) and 0.8 for (**2**) were used, with a 25% extension at each end of the scan range for background determination. The total number of reflections measured was 11 120 for (**1**) and 9 581 for (**2**). No significant decay of the crystal samples was observed upon *X*-ray exposure. The intensities were corrected for Lorentz and polarization effects. An empirical absorption correction was applied to both data sets, based on ψ-scans (ψ 0—360° every 10°) of suitable reflections with χ values close to 90°; the relative transmission factors had values in the ranges 0.97—1.00 for (**1**) and 0.84—1.00 for (**2**), respectively. Two sets of 7 421 [(**1**)] and 3 531 [(**2**)] independent significant reflections, with $I > 3\sigma(I)$, were used in the structure solutions and refinements.

Structure solutions and refinements. All computations were performed on a PDP 11/34 computer, using the Enraf-Nonius Structure Determination Package (SDP) and the physical constants tabulated therein. The structures were solved by direct methods, which showed the locations of the rhodium atoms. Successive difference-Fourier maps revealed the positions of all the non-hydrogen atoms. In compound (**2**) one of the three tetramethylammonium cations was found to be disordered, with three carbon atoms doubled by a rotation of the NC_4 group around one of the N–C bonds. Preliminary refinement of the occupancy of the two models gave approximate values of 65% (unprimed atoms) and 35% (primed ones); these fractions were kept constant in the successive refinements.

The refinements were carried out by full-matrix least-squares methods. Anisotropic thermal parameters were assigned to all the anionic atoms in (**1**) while in (**2**), because of the lower number of significant data, anisotropic factors were assigned to the rhodium atoms only. All the hydrogen atoms were ignored.

The final difference Fourier maps were rather flat showing residual peaks not exceeding *ca.* 1 e $Å^{-3}$ in both cases.

Weights were assigned according to the formula $w = 4F_o^2/\sigma(F_o^2)^2$, where $\sigma(F_o^2) = [\sigma(I)^2 + (pI)^2]^{\frac{1}{2}}/L_p$ (I and L_p are the integrated intensity and the Lorentz-polarization correction, respectively); p was assumed equal to 0.04 for (**1**) and 0.03 for (**2**), respectively. The final values of the conventional agreement indices R and R' were 0.032 and 0.045 for (**1**) and 0.041 and 0.048 for (**2**), respectively.

The final positional parameters are given in Tables 3 and 4.

Table 4. Final positional parameters within $[NMe_4]_3[Rh_{11}(CO)_{23}]\cdot C_6H_5Me$ (**2**)

Atom	*x*	*y*	*z*	Atom	*x*	*y*	*z*
Rh(1)	0.287 57(8)	0.125 6(1)	0.395 53(6)	O(16)	0.148 9(8)	−0.223(1)	0.298 2(6)
Rh(2)	0.185 97(8)	0.208 2(1)	0.312 23(6)	C(17)	0.177(1)	−0.060(2)	0.429 5(8)
Rh(3)	0.238 14(8)	−0.072 3(1)	0.366 68(6)	O(17)	0.157 9(8)	−0.119(1)	0.465 6(6)
Rh(4)	0.140 44(8)	0.010 9(1)	0.292 74(6)	C(18)	0.199(1)	0.021(2)	0.227 1(8)
Rh(5)	0.382 71(8)	0.201 1(1)	0.329 18(6)	O(18)	0.191 1(7)	0.009(1)	0.178 0(5)
Rh(6)	0.288 61(8)	0.284 8(1)	0.252 78(6)	C(19)	0.333(1)	0.139(2)	0.223 8(8)
Rh(7)	0.227 86(9)	0.243 4(1)	0.476 14(6)	O(19)	0.370 7(7)	0.119(1)	0.189 3(6)
Rh(8)	0.143 41(8)	0.323 8(1)	0.396 06(6)	C(20)	0.306(1)	0.419(2)	0.298 8(8)
Rh(9)	0.277 84(8)	0.065 5(1)	0.279 58(6)	O(20)	0.327 6(7)	0.508(1)	0.288 4(6)
Rh(10)	0.277 83(8)	0.337 4(1)	0.364 11(6)	C(21)	0.159(1)	0.377(2)	0.468 4(8)
Rh(11)	0.152 40(8)	0.091 2(1)	0.407 70(6)	O(21)	0.146 6(8)	0.450(1)	0.499 2(7)
C(1)	0.269(1)	−0.213(2)	0.376 9(8)	C(22)	0.151(1)	0.144(2)	0.486 0(8)
O(1)	0.287 8(9)	−0.297(1)	0.383 4(7)	O(22)	0.119 1(8)	0.118(1)	0.525 2(6)
C(2)	0.057(1)	−0.027(2)	0.263(1)	C(23)	0.186(1)	0.425(2)	0.351 7(8)
O(2)	0.001 6(9)	−0.051(1)	0.243 9(7)	O(23)	0.174 1(8)	0.511(1)	0.329 3(6)
C(3)	0.446(1)	0.094(2)	0.317(1)	N(1)	−0.178 0(9)	0.134(1)	0.337 5(7)
O(3)	0.486(1)	0.027(2)	0.312 3(8)	C(T11)	−0.126(1)	0.084(2)	0.300(1)
C(4)	0.440(1)	0.307(2)	0.305(1)	C(T12)	−0.147(2)	0.238(2)	0.350(1)
O(4)	0.477(1)	0.381(2)	0.299 9(9)	C(T13)	0.183(1)	−0.068(2)	0.612(1)
C(5)	0.312(1)	0.355(2)	0.187 3(9)	C(T14)	0.242(2)	0.649(2)	0.193(1)
O(5)	0.328 9(9)	0.398(1)	0.147 7(7)	N(2)	0.501 0(9)	0.313(1)	0.590 1(7)
C(6)	0.249(1)	0.286(2)	0.546 9(9)	C(T21)	0.550(1)	0.292(2)	0.544 7(9)
O(6)	0.259 1(9)	0.320(2)	0.591 9(7)	C(T22)	0.455(1)	0.279(2)	0.094(1)
C(7)	0.051(1)	0.350(2)	0.390 8(9)	C(T23)	0.459(2)	0.096(3)	0.075(1)
O(7)	−0.006 5(9)	0.368(1)	0.390 9(7)	C(T24)	0.537(2)	0.167(3)	0.143(1)
C(8)	0.326(1)	−0.060(2)	0.271 8(9)	N(3)	0.001(1)	−0.310(1)	0.396 9(7)
O(8)	0.356 2(8)	−0.138(1)	0.263 7(6)	C(T31)	−0.002(1)	−0.197(2)	0.383(1)
C(9)	0.323(1)	0.422(2)	0.416 5(9)	C(T32)	0.070(2)	0.142(3)	0.117(1)
O(9)	0.351 6(9)	0.476(1)	0.448 9(7)	C(T33)	0.015(2)	−0.304(4)	0.456(2)
C(10)	0.057(1)	0.074(2)	0.408 5(9)	C(T34)	0.057(2)	0.631(4)	0.372(2)
O(10)	−0.000 6(9)	0.063(1)	0.408 6(7)	C(T32′)	0.070(3)	−0.343(5)	0.423(3)
C(11)	0.332(1)	−0.016(2)	0.398 2(8)	C(T33′)	−0.008(3)	0.150(5)	0.164(3)
O(11)	0.384 8(7)	−0.051(1)	0.412 4(6)	C(T34′)	0.055(6)	0.346(9)	0.580(4)
C(12)	0.383(1)	0.207(2)	0.410 8(8)	C(S1)	0.629(1)	0.213(2)	0.427(1)
O(12)	0.417 2(7)	0.228(1)	0.448 6(6)	C(S2)	0.684(1)	0.229(2)	0.464 5(9)
C(13)	0.291(1)	0.125(2)	0.479 7(9)	C(S3)	0.728(2)	0.321(3)	0.471(1)
O(13)	0.320 6(8)	0.069(1)	0.513 8(6)	C(S4)	0.709(2)	0.395(3)	0.430(1)
C(14)	0.093(1)	0.177(2)	0.301 4(8)	C(S5)	0.658(1)	0.374(2)	0.392(1)
O(14)	0.035 2(7)	0.202(1)	0.290 6(6)	C(S6)	0.612(2)	0.289(3)	0.382(1)
C(15)	0.185 8(9)	0.283(2)	0.241 4(7)	C(S7)	0.589(2)	0.118(3)	0.424(2)
O(15)	0.145 9(7)	0.315(1)	0.206 5(6)				
C(16)	0.166(1)	−0.134(2)	0.312 5(8)				

Acknowledgements

We thank Mrs. M. Bonfa' of Universita' di Milano for recording the n.m.r. spectra.

References

1 A. Fumagalli, S. Martinengo, G. Ciani, and A. Sironi, *J. Chem. Soc., Chem. Commun.*, 1983, 453.
2 M. McPartlin and W. J. H. Nelson, *J. Chem. Soc., Dalton Trans.*, 1986, 1557 and refs. therein.
3 L. J. Farrugia, M. Green, D. R. Hankey, M. Murray, A. G. Orpen, and F. G. A. Stone, *J. Chem. Soc., Dalton Trans.*, 1985, 177.
4 L. Garlaschelli, S. Martinengo, P. L. Bellon, F. Demartin, M. Manassero, M. Y. Chiang, C. Y. Wei, and R. Bau, *J. Am. Chem. Soc.*, 1984, **106**, 6664.
5 R. Bender, P. Braunstein, A. Tiripicchio, and M. Tiripicchio Camellini, *Angew. Chem., Int. Ed. Engl.*, 1985, **24**, 861.
6 S. Martinengo and P. Chini, *Gazz. Chim. Ital.*, 1972, **102**, 344.
7 S. Martinengo, A. Fumagalli, R. Bonfichi, G. Ciani, and A. Sironi, *J. Chem. Soc., Chem. Commun.*, 1982, 825.
8 P. Chini and S. Martinengo, *Inorg. Chim. Acta*, 1969, **3**, 299.
9 S. Martinengo, G. Giordano, and P. Chini, *Inorg. Synth.*, 1980, **20**, 209.
10 L. Garlaschelli, P. Chini, and S. Martinengo, *Gazz. Chim. Ital.*, 1982, **112**, 285.
11 A. Fumagalli, T. F. Koetzle, F. Takusagawa, P. Chini, S. Martinengo, and B. T. Heaton, *J. Am. Chem. Soc.*, 1980, **102**, 1740.
12 S. Martinengo, G. Ciani, and A. Sironi, *J. Chem. Soc., Chem. Commun.*, 1986, 1282.
13 G. Ciani, A. Sironi, and S. Martinengo, *J. Chem. Soc., Chem. Commun.*, 1985, 1757.
14 S. Martinengo, G. Ciani, A. Sironi, and P. Chini, *J. Am. Chem. Soc.*, 1978, **100**, 7096.
15 A. Fumagalli, S. Martinengo, and G. Ciani, *J. Organomet. Chem.*, 1984, **273**, C46.
16 V. G. Albano, D. Braga, and S. Martinengo, *J. Chem. Soc., Dalton Trans.*, 1981, 717.
17 V. G. Albano, D. Braga, and S. Martinengo, *J. Chem. Soc., Dalton Trans.*, 1986, 981.
18 G. Ciani and S. Martinengo, *J. Organomet. Chem.*, 1986, **306**, C49.
19 A. Fumagalli, S. Martinengo, A. Sironi, and G. Ciani, unpublished work.
20 G. Ciani and A. Sironi, *J. Organomet. Chem.*, 1980, **197**, 233.
21 S. Martinengo, G. Ciani, and A. Sironi, *J. Am. Chem. Soc.*, 1982, **104**, 328.
22 B. K. Teo, *Inorg. Chem.*, 1984, **23**, 1251, 1257.
23 C. Allevi, B. T. Heaton, C. Seregni, L. Strona, R. J. Goodfellow, P. Chini, and S. Martinengo, *J. Chem. Soc., Dalton Trans.*, 1986, 1375.
24 B. T. Heaton, L. Strona, S. Martinengo, D. Strumolo, R. J. Goodfellow, and I. H. Sadler, *J. Chem. Soc., Dalton Trans.*, 1982, 1499.

Received 5*th January* 1987; *Paper* 7/019